GSA DATA REPOSITORY 2014070 Byerly et al.

Supplementary Materials

Analytical Methods

Large (>5 cm diameter) samples were disaggregated and 50-150mg of inclusion-free cpx was separated for Lu-Hf analysis. Prior to digestion samples were repeatedly sonicated in 18.2 MΩ water. Samples were digested and Lu and Hf were separated following the methods of (Connelly et al., 2006). Lu and Hf analyses were performed on a VG Isoprobe at the University of Texas at Austin. During Hf analyses ^{173}Yb and ^{175}Lu were measured to account for intereferences on ^{176}Hf. Fractionation was determined according to the ^{179}Hf/^{177}Hf ratio, which was adjusted for the effect from the addition of spike. Hf isotope dilution and isotope composition analyses were performed simultaneously using a ^{180}Hf spike. The average ^{176}Hf/^{177}Hf of JMC475 during the 6-month study was = 0.282181 ± 0.000025 (1σ, n = 25). A solution of BHVO-2 was run as a secondary standard throughout the study and had an average ^{176}Hf/^{177}Hf of 0.283091 ± 0.000014 (1σ, n = 13). Samples are reported relative to the accepted JMC475 value of ^{176}Hf/^{177}Hf = 0.282160. Lu concentrations were determined using a spike enriched in ^{176}Lu. ^{173}Yb and ^{180}Hf were monitored to account for interferences on ^{176}Lu. A fractionation factor was determined based on ^{171}Yb/^{173}Yb and a correction factor was applied to account for the difference in fractionation between Yb and Lu. Cpx Nd analyses and spinel major element analyses were performed following the methods of (Byerly and Lassiter, 2012). Neodymium was run as a metal on double Re filaments using the Triton TIMS at the University of Texas at Austin. The AMES-1 standard was run frequently in between samples and produced an average ^{143}Nd/^{144}Nd of 0.512070 ± 0.000010 (2 s.d.). Methods for Sr and Pb analyses can be found in (Byerly and Lassiter, 2012). Blanks were <30pg for Nd, <40pg for Hf, and <5pg for Lu.

pMELTS Models

In order to model the adiabatic ascent and melting of mantle with different bulk compositions we utilized pMELTS software (Ghiorso et al., 2002). We used the average bulk-composition of the Elephant Butte xenoliths to estimate the melt productivity of fertile mantle with ultra-depleted isotopic compositions. In order to simulate the major element composition of ultra-depleted domains from the Gakkel ridge and Hawai'i we subtracted varying amounts of MORB (Workman and Hart, 2005) from a primitive mantle composition (McDonough and Sun, 1995) until we reached the average bulk-Al_2O_3 composition of the respective localities. Those bulk compositions were entered into the pMELTS software to model adiabatic ascent and melting. The bulk compositions were initially equilibrated at 1375°C and 25kb at the FMQ buffer. The initial temperature of 1375°C was chosen to correspond to a potential temperature of

~1350°C (Lee et al., 2009). The samples were then brought up isentropically to 2kb without constraint on $f\,O_2$ while fractionating any liquid that was produced. The results of these models are shown below.

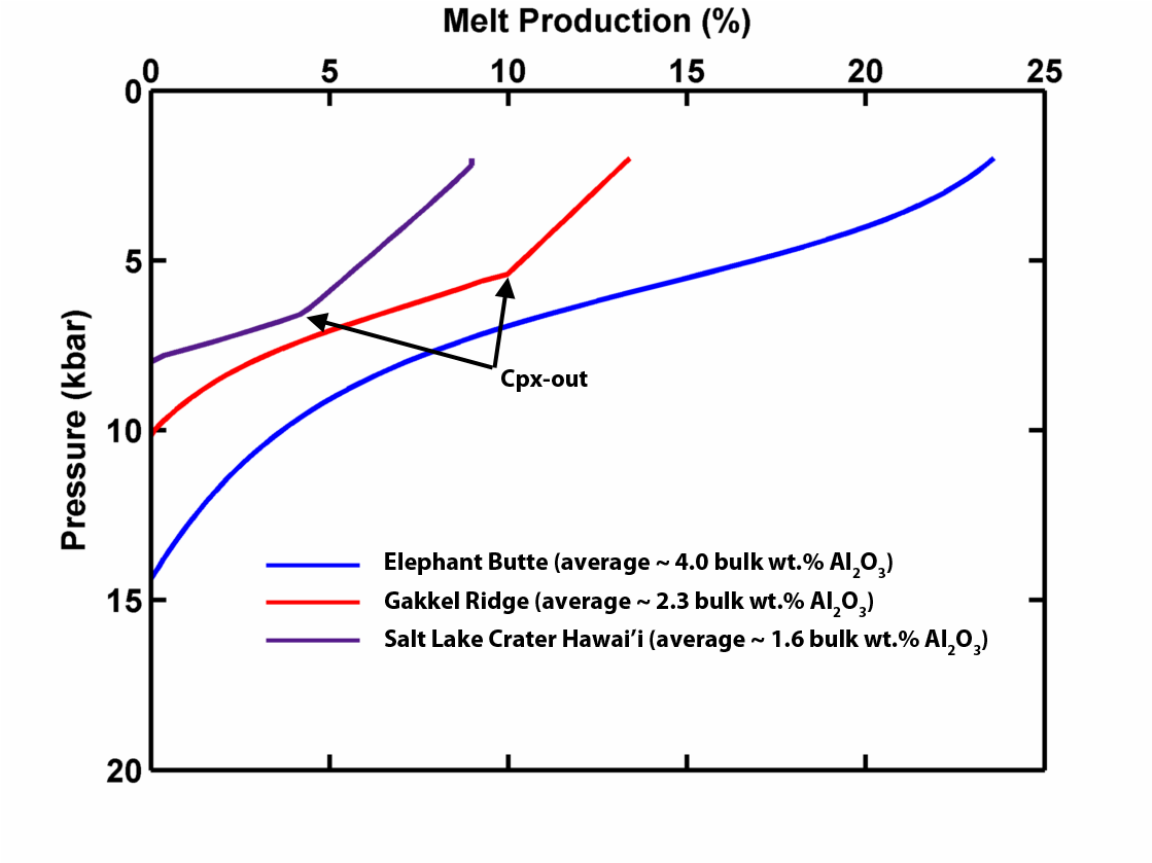

Figure DR1. Results of pMELTS models for the adiabatic ascent and melting of ultra-depleted mantle with different starting bulk compositions. The amount of melt produced is strongly controlled by the starting composition. Despite their moderately refractory to refractory compositions, samples from Hawai'i and the Gakkel ridge are capable of producing melt.

The results of these models suggest that very fertile (> 3.5wt. % Al_2O_3) ultra-depleted domains, such as those from Elephant Butte, may be under-sampled by abyssal peridotites due to some degree of recent melt extraction. Abyssal peridotites sample the top of the adiabatic melting column beneath a mid-ocean ridge (~2.2kb) and could have experienced up to 15-20% melt extraction subsequent to their emplacement on the seafloor, whereas samples derived from ~40km depth would have experienced very little (<5%) melt extraction in the same melting column.

Mixing of Eclogite Component

We chose our eclogite component to be derived from MORB that was subducted into the mantle 2.0 Ga. We assumed the MORB at 2 Ga to have the same isotopic composition as DMM at 2 Ga (using Lu/Hf, Sm/Nd, $^{143}Nd/^{144}Nd$, and $^{176}Hf/^{177}Hf$ of DMM from Workman and Hart, 2005). We also assumed MORB generated at 2Ga to have the same composition as average MORB today (Keleman et al., 2007). During subduction neither the isotopic compositions nor parent/daughter ratios are disturbed. This subducted MORB component then remains chemically isolated from the rest of the mantle for 2Ga while undergoing radiogenic in-growth to yield its present-day composition. The weighted mean Hf and Nd isotopic compositions of the Elephant Butte xenoliths were used along with average Hf and Nd concentrations from the Elephant Butte xenoliths. The average Elephant Butte mantle component was mixed with the 2 Ga MORB component to generate the mixing curve in Figure 2B.

Inputs to Mixing Model

	Nd (ppm)	$^{143}Nd/^{144}Nd$	ε_{Nd}	Hf (ppm)	$^{176}Hf/^{177}Hf$	ε_{Hf}
Elephant Butte	0.53	0.513358	14.0	0.15	0.283474	24.8
MORB-derived eclogite	9.3	0.512327	-6.1	2.31	0.282211	-19.8

Preferential Sampling of Fertile Mantle Components

The pMELTS models describe above demonstrate that a range of source compositions are capable of melting when advected along a modern mantle adiabat. In a heterogeneous mantle, melts brought to the surface represent a sum of melts generate by melting sources with a range of fertilities and incompatible trace element compositions. Because the fertile components melt more, melt over a larger depth range, and have higher incompatible trace element concentrations, the melts generated from a heterogeneous mantle will be biased towards these fertile compositions. To demonstrate this effect we have performed a Monte Carlo simulation to model the compositions of melts that would be generated from a heterogeneous mantle. We took primitive mantle (McDonough and Sun, 1995) and extracted variable amounts of melt at 2 Ga. This ancient melting results in a wide range of major element compositions and isotopic compositions in the mantle (Figure DR2). This mantle is brought up adiabatically and melts

following the pMELTS models described above. The amount of melting, and depth at which melting initiates is a function of the fertility of the source (e.g. Figure DR1). For simplicity we summed the melts generated from five discrete intervals in a triangular melting region. In the scenario shown in Figure DR2, an average of 9 ± 0.3 (1σ) % melt was extracted from primitive mantle to generate the source mantle. This results in an average bulk composition of ~3.2 ± 0.5 (1σ) wt. % Al_2O_3 which ranges from ~4.4 to ~1.3 wt. Al_2O_3. The 2Ga time integrated effect of this melt depletion results in a mantle with a weighted mean ε_{Hf} of ~44. However, the melts generated from melting this mantle in a triangular melt region have ε_{Hf} of ~29 (Figure DR2). This is due to the large proportion of melt generated by more fertile (and less depleted) components. The melts appear the represent a mantle that is considerable less-depleted than the actual source composition.

Salters and Stracke (2004) estimate the major element composition of DMM by subtracting a small amount (1.5% total from two different pressures) of melt from PM. Their constraints on the amount of melt extracted are the isotopic compositions and parent/daughter ratios of their estimate for DMM. This method underestimates the average amount of melt extraction from PM due to MORB melts having less depleted compositions than the actual average mantle source if the mantle is compositionally heterogeneous on the scale sampled at mid-ocean ridges.

Workman and Hart (2005) estimate major the element of DMM by determining the modal abundances of mantle minerals that correspond to their estimate for the trace element composition of MORB (via correlations between modal abundances and incompatible trace elements in abyssal peridotites). They too encounter the same problem that MORB preferentially sample the most fertile (and least depleted) mantle. Therefore, since their estimate for DMM is not as depleted in incompatible trace elements as “average” peridotitic convecting upper mantle they overestimate the fertility of DMM.

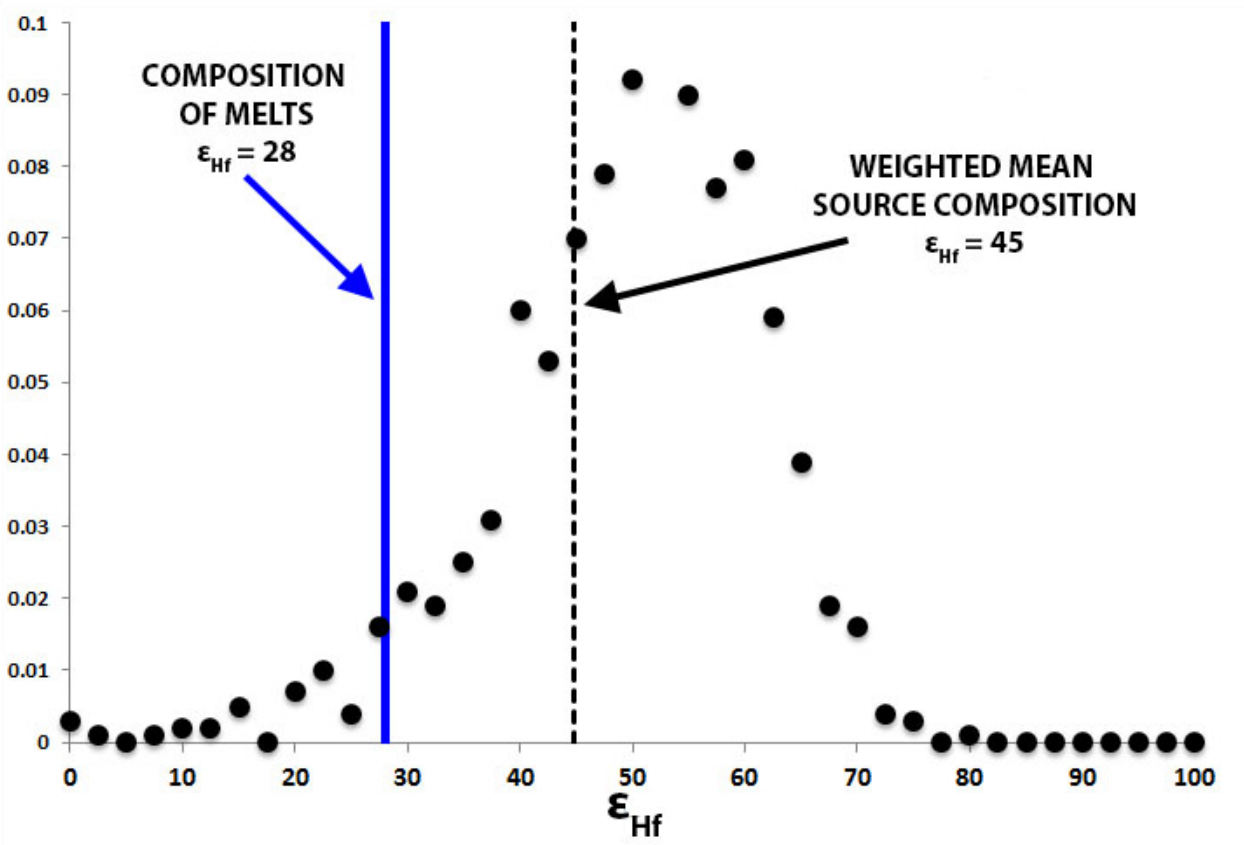

Figure DR2. Monte Carlo simulation demonstrating the distribution of mantle hafnium isotopic compositions resulting from variable (9 ± 3 (1σ) %) melt extraction from primitive mantle at 2 Ga (black circles). The weighted mean hafnium composition of the mantle source at present day is shown as a dashed black line. The melts extracted from this mantle source have a less-depleted isotopic composition (solid blue line)

Table DR1 Input compositions and results of pMELTS models

Starting Compositon	SiO_2	Al_2O_3	FeO^T	MnO	MgO	CaO	Na_2O	Cr_2O_3	TiO_2
Average Elephant Butte	44.69	4.03	8.43	0.15	38.52	3.45	0.24	0.37	0.13
Gakkel Ridge [a]	44.24	2.28	8.05	0.13	42.79	1.97	0.04	0.44	0.08
Salt Lake Crater Hawai'i [b]	43.94	1.56	8.05	0.13	44.39	1.44	0.00	0.45	0.04

[a] Bulk composition was estimated by removing MORB from PM to reach ~2.3 wt.% Al_2O_3 (average of Gakkel Ridge peridotites)

[b] Bulk composition was estimated by removing MORB from PM to reach ~1.6 wt.% Al_2O_3 (average of SLC Hawai'i xenoliths)

Accumulated Melts	SiO_2	Al_2O_3	FeO^T	MnO	MgO	CaO	Na_2O	Cr_2O_3	TiO_2
Average Elephant Butte	49.78	16.05	8.53	0.01	12.00	11.77	1.03	0.03	0.54
Gakkel Ridge	50.58	14.79	8.45	0.01	13.23	11.74	0.30	0.04	0.57
Salt Lake Crater Hawai'i	53.19	14.48	6.77	0.01	13.11	11.83	0.00	0.09	0.41

Residue	SiO_2	Al_2O_3	FeO^T	MnO	MgO	CaO	Na_2O	Cr_2O_3	TiO_2
Average Elephant Butte	43.08	0.34	8.39	0.19	46.60	0.90	0.00	0.47	0.00
Gakkel Ridge	43.23	0.36	7.98	0.15	47.29	0.47	0.00	0.50	0.00
Salt Lake Crater Hawai'i	43.03	0.29	8.17	0.14	47.45	0.42	0.00	0.49	0.00

Table DR2

	$^{87}Sr/^{86}Sr$	$^{206}Pb/^{204}Pb$	$^{207}Pb/^{204}Pb$	$^{208}Pb/^{204}Pb$	$^{143}Nd/^{144}Nd$	εNd	Nd (ppm)	$^{47}Sm/^{144}Nd$	$^{176}Hf/^{177}Hf$	εHf	Hf (ppm)	$^{176}Lu/^{177}Hf$	spinel Cr#
[a] **07EB1.01**	0.701756	17.99	15.39	37.46	0.514017	26.9	2.24	0.34	0.283892	39.6	0.72	0.045	0.108
07EB1.05	0.702644				0.513094	8.9	2.72	0.32	0.283267	17.5	1.17	0.034	0.091
[a] **07EB1.09**	0.701857	18.20	15.47	37.52	0.513223	11.4	4.75	0.26					0.085
07EB2.03	0.702091				0.513466	16.2	3.54	0.29	0.283580	28.6	0.98	0.039	0.106
[a] **07EB4.01**	0.702518	18.61	15.53	38.00	0.513067	8.4	4.55	0.27	0.283104	11.7	1.17	0.031	0.082
[a] **07EB4.05**	0.702164	19.07	15.46	38.48	0.513168	10.3	3.71	0.26	0.283223	15.9	1.04	0.037	0.093
[a] **07EB4.21**	0.701778	18.31	15.43	37.88	0.513717	21.1	1.35	0.43	0.283541	27.2	0.52	0.061	0.111
BELB 4-1	0.702403				0.513258	12.1	4.17	0.24	0.283400	22.2	0.96	0.039	0.112
[a] **BELB 5-1**	0.701877	18.39	15.41	37.58	0.513340	13.7	2.50	0.34					0.103
BELB 5-5	0.702100				0.513688	20.5	3.11	0.30	0.283748	34.5	0.87	0.048	0.096
[a] **BELB 5-8**	0.701986	18.47	15.48	37.25	0.513273	12.4	3.70	0.27	0.283213	15.6	1.02	0.047	0.084
BELB 9-6					0.513612	19.0	2.90	0.30	0.283880	39.2	0.74	0.045	0.109
[a] **BELB 9-8**	0.702271	18.49	15.42	37.83	0.513380	14.5	2.31	0.35	0.283351	20.5	0.72	0.054	0.110

[a] Sr, Nd, and Pb isotopic data from Byerly and Lassiter, 2012

References Cited

Byerly, B.L., and Lassiter, J.C., 2012, Evidence from mantle xenoliths for lithosphere removal beneath the central Rio Grande Rift: Earth and Planetary Science Letters, v. 355–356, p. 82–93, doi:10.1016/j.epsl.2012.08.034.

Connelly, J., Ulfbeck, D., Thrane, K., Bizzarro, M., and Housh, T., 2006, A method for purifying Lu and Hf for analyses by MC-ICP-MS using TODGA resin: Chemical Geology, v. 233, p. 126–136, doi:10.1016/j.chemgeo.2006.02.020.

Ghiorso, M.S., Hirschmann, M.M., Reiners, P.W., and Kress, V.C., III, 2002, The pMELTS: A revision of MELTS for improved calculation of phase relations and major element partitioning related to partial melting of the mantle to 3 GPa: Geochemistry Geophysics Geosystems, v. 3, no. 5, p. 1–35, doi:10.1029/2001GC000217.

Kelemen, P.B., Hanghøj, K., and Greene, A.R., 2007, One view of the geochemistry of subduction-related magmatic arcs, with an emphasis on primitive andesite and lower crust, in Heinrich, D.H., and Karl, K.T., eds., Treatise on Geochemistry: Oxford, UK, Pergamon, p. 1–70.

Lee, C.-T. A., Luffi, P., Plank, T., Dalton, H., and Leeman, W. P., 2009, Constraints on the depths and temperatures of basaltic magma generation on Earth and other terrestrial planets using new thermobarometers for mafic magmas: Earth and Planetary Science Letters, v. 279, p. 20–33, doi:10.1016/j.epsl.2008.12.020.

McDonough, W.F., and Sun, S.S., 1995, The composition of the Earth: Chemical Geology, v. 120, p. 223–253, doi:10.1016/0009-2541(94)00140-4.

Salters, V.J.M., and Stracke, A., 2004, Composition of the depleted mantle: Geochemistry Geophysics Geosystems, v. 5, Q05B07, doi:10.1029/2003GC000597.

Workman, R.K., and Hart, S.R., 2005, Major and trace element composition of the depleted MORB mantle (DMM): Earth and Planetary Science Letters, v. 231, p. 53–72, doi:10.1016/j.epsl.2004.12.005.